ISBN: 978-3-95450-204-2 ISSN: 2673-5350 doi:10.18429/JACoW-IBIC2019-MOPP047

DESIGN AND DEVELOPMENT OF BEAM DIAGNOSTICS FOR AN FETS-FFA RING FOR ISIS-II UPGRADE STUDIES

E. Yamakawa*, JAI in Oxford University, Oxford, United Kingdom
C. C. Wilcox, A. Pertica, S. Machida, RAL STFC, Didcot, United Kingdom

Abstract

The ISIS-II project aims to deliver a new spallation neutron source by 2034, driven by a 1.2 GeV proton accelerator capable of delivering a beam power of 1.25 MW with a repetition rate of 50 Hz or higher. One of the options for this future accelerator is a Fixed Field alternating gradient Accelerator (FFA). To demonstrate the suitability of FFAs for use in a user facility such as ISIS, there is a plan to construct a smaller scale proof of concept machine: FETS-FFA. Developing beam diagnostics for the FETS-FFA ring presents a challenge due to a large orbit excursion and aperture (60 mm x 700 mm). Diagnostics must cover the full size of beam chamber whilst still providing measurement sensitivity and resolution comparable to that seen in the ISIS synchrotron.

This paper presents the current design and development of beam diagnostics for the FETS-FFA ring, including finite element studies of Beam Position Monitors and Ionisation Profile Monitors.

INTRODUCTION

The feasibility studies for an intensity upgrade of ISIS, towards a 1.25 MW proton driver for neutron provision in Europe, was started in 2016 [1]. One of the options being considered is a Fixed Field Alternating gradient (FFA) ring [2, 3]. FFAs utilise static magnetic fields to accelerate a particle beam with a high repetition rate (~200 Hz), while achieving high beam intensities. In order to demonstrate the viability of an FFA for a high intensity user facility, the small-scale FETS-FFA ring will be built initially, before the final decision is made on which type of accelerating ring will be used in ISIS-II. The preliminary parameters of FETS-FFA are summarised in Table 1.

Table 1: Preliminary parameters of FETS-FFA ring

Beam energy range	3 - 30 MeV
Central radius	4 m
Orbit excursion	0.58 m
Bunch intensity N_p	10^{10} ppb
Harmonic number	2
RF bandwidth	4 - 7 MHz
Bunch length at 3 MeV, 30 MeV ($4\sigma_L$)	31 ns, 54 ns

A key challenge in the development of beam diagnostics for this ring (and other FFA's) is the requirement to measure across the large beam chamber width (~700 mm) whilst also achieving high measurement sensitivity and resolution, comparable to those achieved in the ISIS synchrotron. In this paper, the current designs of a Beam Position Monitor (BPM) and Ionisation Profile Monitor (IPM) for FETS-FFA are presented.

* emi.yamakawa@physics.ox.ac.uk

BEAM POSITION MONITOR DEVELOPMENT

BPM development for the FETS-FFA ring has focused on a rectangular, electrostatic shoe-box type monitor (also known as a split-plate BPM) [4], with two pairs of electrodes to allow measurement in both the horizontal and vertical planes. This type of BPM has been installed and demonstrated in a proof-of principle FFA at KEK, in 2001 [5], and is the same style as the BPMs used at ISIS [6].

Assuming the beam is centred in a rectangular vacuum chamber, the maximum detected pick-up signal ($V(t)$) [4] is given by:

$$V(t) = \frac{1}{c\beta C}\frac{A}{2\pi(a+b)/4} I_{\text{beam}}(t), \quad (1)$$

where c is the speed of light, C the capacitance between the electrode and ground, A the area of the electrode, I_{beam} the beam current, a the vertical electrode separation and b the horizontal electrode separation. When measuring this voltage, the BPM acts as a first order high-pass filter, with a cutoff frequency given by $f_{\text{cut}} = 1/2\pi RC$. As a result, the termination impedance which the signal is measured across must be high, in order to give a low enough cutoff frequency for the bandwidth requirement of the FETS-FFA ring, as listed in Table 1.

The FETS-FFA ring requires such a large vacuum chamber because the beam orbit moves as the beam energy increases, over a range of about 600 mm. The preliminary design of the ring includes several straight vacuum chambers between each main magnet, and it is within these sections that the beam diagnostics will be installed. Each straight section is 0.75 m long, with an internal aperture of 778 mm × 138 mm, meaning any installed BPMs must have very large widths. Preliminary designs of the monitor have apertures of 710 mm × 70 mm, and electrode thicknesses of 4 mm. Figure 1 shows the preliminary design of the BPM, rendered in CST electromagnetic finite element software [7]. Inside the vacuum chamber, each electrode pair is formed by splitting a rectangular shaped electrode with a diagonal cut. This cut means that offsets in beam position from the centre of the monitor induce different strength signals on each electrode, yielding a beam position measurement. Electrical coupling between adjacent electrodes can reduce the measurement accuracy and sensitivity of these monitors, and this problem is exacerbated by the large electrode size required. To mitigate this, earthed guard-rings (the blue material in

ISBN: 978-3-95450-204-2 ISSN: 2673-5350 doi:10.18429/JACoW-IBIC2019-MOPP047

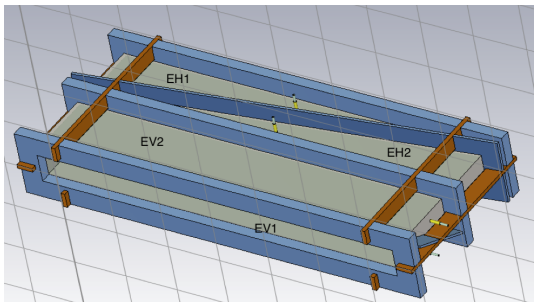

Figure 1: 3D CST model of the preliminary BPM design. The electrode pairs are named EH1,2 and EV1,2 for the measurement of horizontal and vertical position respectively.

Fig. 1) are placed in the gaps between adjacent electrodes, electrically isolating them from each other. Lastly, PEEK supports are used to fix the BPM assembly to the vacuum chamber (the orange material in Fig. 1).

As presented in Eq. (1), the amplitude of the signal induced on an electrode by a beam current is affected by the capacitance between the electrode and the earthed vacuum chamber. As the beam position is obtained by comparing the signals in each electrode pair (e.g. EH1 and EH2 for horizontal position), the sensitivity of each electrode to the beam current must be uniform for accurate measurements to be taken. Therefore, the electrode-earth capacitances within each pair should also be uniform. Uneven capacitances result in the electrical centre of the monitor being different to the mechanical centre, introducing an offset error, δ, into the measurements.

To calculate the capacitance of each electrode, electromagnetic field simulations were carried out with CST EM Studio. In the simulations, a 1 V static potential was applied to a cylindrical pipe, placed along the beam axis of the vacuum chamber, while the rest of the components were grounded. The results are shown in Table 2, and show closely matched capacitances within each electrode pair. The capacitances in the horizontal electrode pair (EH1 and EH2) are different to the vertical pair (EV1 and EV2) due to the difference in size between each section of the BPM.

Table 2: Simulated capacitances between each electrode and ground.

EH1	EH2	EV1	EV2
120 pF	119 pF	96.9 pF	96.9 pF

The monitor's sensitivity to changes in beam position was also optimised using CST EM Studio. The potential induced on each electrode was computed while the horizontal and vertical position of the cylindrical pipe, used to imitate the beam, were varied. The pipe had a 1 V static potential applied to it, ensuring a potential could be measured on each electrode, while both the guard-rings and vacuum chamber were grounded.

When considering a single electrode pair, the beam displacement from the centre of the BPM, x, is related to the difference over the sum of the signals induced on each electrode, $U_{1,2}$, by the monitor's position sensitivity, S, such that:

$$\frac{U_2 - U_1}{U_1 + U_2} = S \cdot x + \delta. \quad (2)$$

The position sensitivity of an ideal BPM is inversely proportional to the internal width of the electrodes, W, such that $S_{\text{ideal}} = 2/W$. As a result, the ideal sensitivity for the FETS-FFA BPM is 0.0028 mm^{-1} in the horizontal plane and 0.033 mm^{-1} in the vertical plane. If the electrical coupling between adjacent electrodes is not mitigated, the sensitivity of a BPM will fall below this ideal value. This is prevented with the use of earthed guard rings to electrically isolate each electrode in the BPM.

Figure 2 shows the variation of the difference over sum values for each pair of electrodes, calculated in CST, as the beam was moved along the monitor's horizontal and vertical axes. A line of best fit is calculated for each plane, with the gradient giving the sensitivity of the BPM. The y-intercept value gives the beam offset error (δ), which is constant regardless of beam position. As shown in Fig. 2, inter-electrode coupling in both the horizontal and vertical sections of the monitor is well mitigated, and the position sensitivity is very close to the ideal values stated above. In both planes the offset error is also very low, as expected from the well-matched capacitances shown in Table 2.

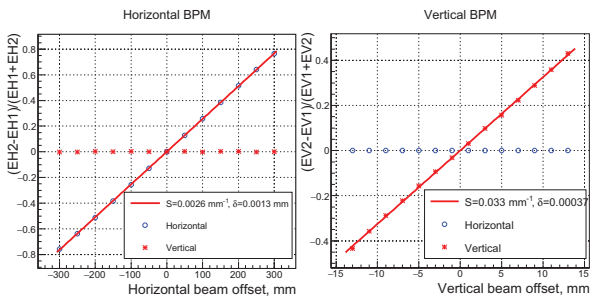

Figure 2: Difference over sum plots for the horizontal and vertical sections of the BPM, along with their associated sensitivity values. The linear fitting function presented by Eq. (2). was applied to estimate sensitivity and offset error.

The impact of varying the angle of the cut between the horizontal electrodes on both capacitance and position sensitivity was also analysed. Figure 3 shows effect of varying this angle on both electrode capacitance to earth and horizontal position sensitivity. Increasing the cut angle results in an increased electrode-earth capacitance. However, position sensitivity converges at about 8 degrees of cut angle, remaining roughly constant if the angle is increased beyond this. To maximise the output signal, a balance between capacitance and sensitivity must be found, and these plots confirm that for the preliminary design, a cut angle of 7.96° is optimal. To accommodate these optimised angles, different overall longitudinal lengths are used for the electrode pairs within the horizontal and vertical sections of the monitor.

ISBN: 978-3-95450-204-2 ISSN: 2673-5350 doi:10.18429/JACoW-IBIC2019-MOPP047

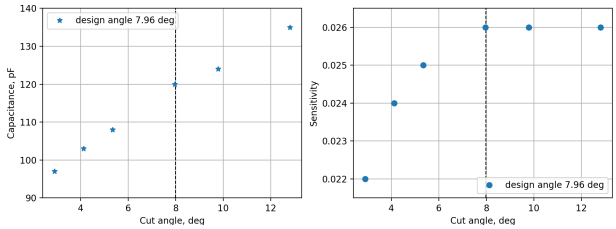

Figure 3: Variation of the horizontal BPM electrode capacitances to earth (left) and beam position sensitivity (right) with the cut angle between the electrode pair.

IONISATION PROFILE MONITOR DEVELOPMENT

In existing FFA machines, the beam profile is measured destructively by inserting phosphor screens into the path of the beam. Non-destructive profile monitors have not yet been demonstrated in an FFA, but would be beneficial for taking turn-by-turn measurements during operation. For the FETS-FFA ring, an ionisation profile monitor (IPM) is under development to provide such non-destructive beam profile monitoring. IPMs measure the beam profile by collecting residual gas ions (or electrons) generated as the beam interacts with particles in the beam pipe vacuum. A drift field is generated across the monitor aperture by applying a high voltage to an anode plate, which guides these particles towards a charged particle detector positioned on the opposite side of the monitor. FETS-FFA IPMs will operate by guiding and detecting residual gas ions, to avoid needing to install huge magnets around the beam pipe, which are required to provide guiding fields if electrons are used [8].

The preliminary horizontal and vertical IPM designs each contain an anode on one side of the beam aperture, with a positive potential applied to generate the ion drift field, and an earthed plate on the opposite side for the detectors to be mounted on, as shown in Fig. 4. Between the anode and grounded plate, a set of additional "shaping-field" electrodes are placed along the sides of the beam aperture to ensure the drift field has a uniform transverse shape within the monitor [9]. The charged particle detectors will be placed on ceramic housing, attached to the grounded plate. While the final choice of detector has not yet been decided, an array of Channeltron 4800 series electron multipliers [10] is the most likely option, primarily due to their long lifespan and successful use in the existing ISIS IPMs.

Assuming that hydrogen gas is the main particle present in the FETS-FFA ring, the number of ion-electron pairs generated, N, by a proton beam of energy E, within a monitor of length dZ, can be estimated by [11]:

$$N = N_p \rho P \frac{dE}{dx} \frac{1}{W} dZ, \tag{3}$$

where P is the vacuum pressure, dE/dx the stopping power in hydrogen of protons at the beam energy, W the mean energy required to produce a hydrogen ion-electron pair and ρ the molecular density of hydrogen. Assuming a vacuum level of 10^{-5} Pa, approximately 13,000 ion-electron pairs are expected to be generated at 3 MeV (injection energy), and 2,000 pairs at 30 MeV (extraction energy). This is significantly lower than the ~150.000 pairs generated in the existing ISIS IPMs, meaning the measured profile signal will be both weaker and more susceptible to random fluctuations in the measurement.

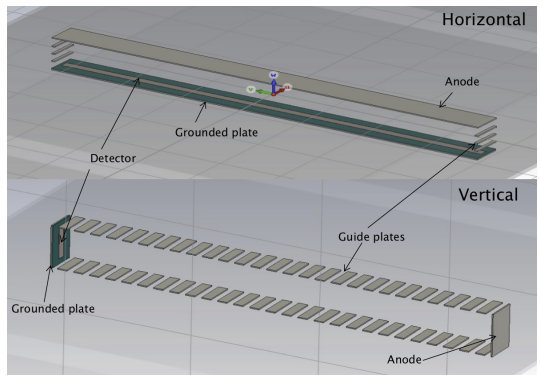

Figure 4: Simplified CST models of the horizontal (top) and vertical (bottom) IPMs for the FETS-FFA ring. The anode and grounded plate of the horizontal IPM have surface areas of 710 mm × 5 mm, thicknesses of 2 mm and are separated by 60 mm. For the vertical IPM, the anode and grounded plate have surface areas of 80 mm × 5 mm, thicknesses of 2 mm and are separated by 710 mm. The ion detectors have a total surface area of 700 mm × 14 mm in the horizontal IPM and 60 mm × 14 mm in the vertical IPM.

One characteristic of FFA operation is that the orbit increases with the beam energy. Therefore, obtaining accurate profiles requires single turn measurements to be taken, to prevent ions generated from consecutive orbits overlapping and reaching the detectors at the same time. For each IPM design, the trajectories of beam-generated ions were computed using particle tracking simulations, carried out with CST Particle Studio's tracking solver. The anode voltages were set to 10 kV and 1 MV in the horizontal and vertical monitors respectively. These values were chosen as they are the values required to guide the ions to the detectors within the revolution time of the ring, which is approximately 200 ns. From these values, it is clear that a turn-by-turn vertical IPM measurement is not realistic for the FETS-FFA ring, due to the large beam pipe aperture in this plane.

In order to generate an approximate beam space charge field in the CST particle simulations, a 2 m-long cylindrical pipe made of vacuum was created, consisting of 4 layers of increasing radii: σ, 2σ, 3σ and 4σ, where $\sigma = 4$ mm. Each layer had a proportion of the bunch charge distributed uniformly across its surface, with the charge applied to each layer calculated as:

$$Q(x) = N_p q_e \frac{A_x}{A_t} \frac{L_x}{L_t}, \tag{4}$$

where q_e is the elementary charge, A_x the cross section of each layer, A_t the cross section of the 4σ beam layer (i.e. the outer layer), L_x the beam length in CST (2 m) and L_t

ISBN: 978-3-95450-204-2 ISSN: 2673-5350 doi:10.18429/JACoW-IBIC2019-MOPP047

the bunch length for $4\sigma_L$ (6.86 m for 3 MeV and 4 m for 30 MeV). H_2^+ ions were generated on the outer layer of the beam cylinder, along a 16.7 mm length (longitudinally), centred on the IPM detectors. Ions generated outside of this smaller length would not be guided into the IPM detectors, so would not affect the measured profile, and would vastly increase computation time if they were included in the simulation.

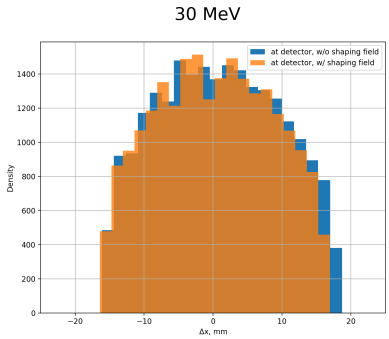

Figure 5: Histogram plots of detected profiles with and without shaping fields at 30 MeV proton beam energy. Δx is the displacement from the beam centre.

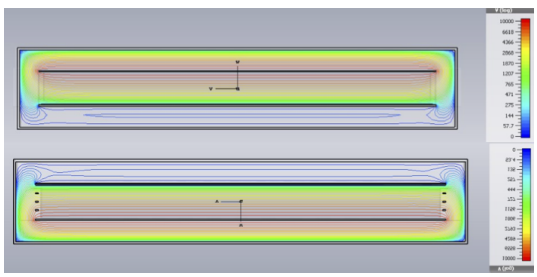

Figure 6: Transverse cross sections showing electric potential contours in the horizontal IPM without (top) and with (bottom) the shaping field. Potentials near the monitor edges are distorted unless the shaping fields are present. In both plots, the beam space charge field is not taken into account.

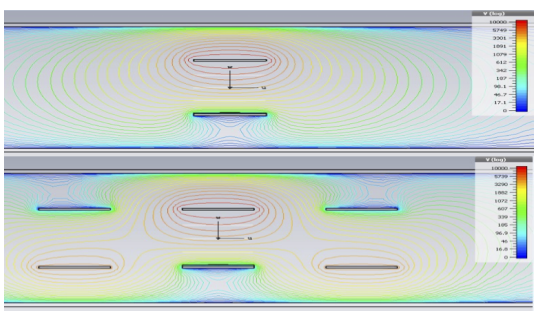

Figure 7: Cross sections of the monitor, showing the longitudinal electric potential (along beam direction) without (top) and with (bottom) the compensating fields. The bias potential on the IPM anode is 10 kV, while the bias on each compensating electrodes is 5 kV.

In the tracking simulation, the initial velocity of the beam-generated ions was set to zero. Figure 5 shows the ion profiles measured by the horizontal IPM, with and without the shaping field active. As the beam pipe and drift field anode are so large, the drift field is uniform in the centre of the monitor regardless of whether the shaping fields are powered. However, at the beam energy extremes of both 3 and 30 MeV, the beam orbit is close to the edge of the anode, where the drift field shape is affected by the earthed vacuum chamber walls (shown in Figs. 6 and 7). This effect is larger nearer to the beam pipe walls, and consequently at these energies the measured ion profile becomes asymmetric with respect to the beam centre if the shaping field is not active, as the drift field guides ions towards the earthed beam pipe walls in addition to guiding them towards the detectors.

In addition to guiding ions towards the IPM detectors, the drift field applies an unwanted kick to the FFA beam as it passes through the monitor. To compensate for this, two additional pairs of electrodes have been added to the preliminary design, one pair upstream and the other downstream of the monitor, each separated by 50 mm. These will provide compensating fields to ensure there is no net kick applied to the beam. Further simulation studies will be performed in the future, using more realistic beam and ion distributions and a custom particle tracking code which has been written for the ISIS IPMs.

CONCLUSIONS AND FUTURE WORK

Preliminary designs for a BPM and IPM have been produced for the ISIS FETS-FFA ring. In both cases, the extremely large beam pipe aperture poses the main challenge when designing these monitors.

BPM design parameters have been optimised with CST simulations. The monitor's beam position sensitivity has been maximised, while signal coupling between adjacent electrodes has been well-suppressed using earthed guard rings placed between each electrode. At the time of writing, a prototype 4-electrode BPM, which has been scaled down to half the width of preliminary design, is being manufactured to enable bench measurements to be carried out and to verify the design simulations presented in this paper.

It has been determined that a vertical IPM is not a feasible option for the FETS-FFA ring, as the large aperture requires approximately 1 MV to be applied to the drift field anode, which is not realistic. On the other hand, a horizontal IPM only requires an anode potential of 10 kV to guide the residual gas ions sufficiently. Potential distortion of the measured profile by a non-uniform drift field has been mitigated with the use of additional shaping field electrodes. The use of additional compensating fields has been considered, to prevent the IPM applying a kick to the beam as it passes through the monitor. Further simulation work will be performed to study these effects in more detail, using more realistic beam charge distributions and including the affect of magnetic fringing fields of main magnets located near to the monitor.

REFERENCES

[1] J.-B. Lagrange *et al.*, "Progress on Design Studies for the ISIS II Upgrade", in *Proc. 10th Int. Particle Accelerator Conf.*

ISBN: 978-3-95450-204-2 ISSN: 2673-5350 doi:10.18429/JACoW-IBIC2019-MOPP047

(IPAC'19), Melbourne, Australia, May 2019, pp. 2075–2078. doi:10.18429/JACoW-IPAC2019-TUPTS068

[2] T. Ohkawa, Proc. annual meeting of JPS, 1953.

[3] K. R. Symon, D. W. Kerst, L. W. Jones, L. J. Laslett, and K. M. Terwilliger, "Fixed-Field Alternating-Gradient Particle Accelerators", *Phys. Rev.*, vol. 103, Sep. 1956., p. 1837. doi:10.1103/PhysRev.103.1837

[4] P. Forck, P. Kowina, and D. Liakin, "Beam Position Monitors", CAS - CERN Accelerator School: Course on Beam Diagnostics, Dourdan, France, May - Jun 2008, p. 187. doi:10.5170/CERN-2009-005

[5] M. Yoshimoto *et al.*, "Recent Beam Studies of the POP FFAG Proton Synchrotron", in *Proc. 19th Particle Accelerator Conf. (PAC'01)*, Chicago, IL, USA, Jun. 2001, paper MOPA012, pp. 51–53. doi:10.1109/PAC.2001.987429

[6] C. C. Wilcox, J. C. Medland, S. J. Payne, A. Pertica, and M. A. Probert, "Optimisation of a Split Plate Position Monitor for the ISIS Proton Synchrotron", in *Proc. 2nd Int. Beam Instrumentation Conf. (IBIC'13)*, Oxford, UK, Sep. 2013, paper WEPC25, pp. 739–741.

[7] 3-dimensional electromagnetic field simulation software. https://cst.com

[8] D. Vilsmeier, M. Sapinski, and R. Singh, "Space-charge distortion of transverse profiles measured by electron-based ionization profile monitors and correction methods", *Phys. Rev. Accel. Beams*, vol. 22, May 2019, p. 05280. doi:10.1103/PhysRevAccelBeams.22.052801

[9] C. C. Wilcox, B. Jones, A. Pertica, and R. E. Williamson, "An Investigation into the Behaviour of Residual Gas Ionisation Profile Monitors in the ISIS Extracted Beamline", in *Proc. 5th Int. Beam Instrumentation Conf. (IBIC'16)*, Barcelona, Spain, Sep. 2016, pp. 807–810. doi:10.18429/JACoW-IBIC2016-WEPG68

[10] Photonis, https://www.photonis.com

[11] K. Satou and T.M. Mitsuhashi, "Simulation and Progress in Ionization Profile Monitors for High Intensity Proton Beam", presented at the 6th Int. Beam Instrumentation Conf. (IBIC'17), Grand Rapids, MI, USA, Aug. 2017, paper WE3AB2, unpublished.